

## Thermal Fatigue Behavior of Asphalt Concrete: A Laboratory-based Investigation Approach

Ali Arabzadeh<sup>1</sup> and Murat Guler<sup>2\*</sup>

<sup>1</sup>Graduate Research Assistant, 176 Town Engineering Building, Department of Civil, Construction and Environmental Engineering, Iowa State University, Ames, IA 50011, USA, Phone: +1-515-708-4621, E-mail: [arab@iastate.edu](mailto:arab@iastate.edu)

<sup>2</sup>Professor, 401 K1 Building (**corresponding author\***), Department of Civil Engineering, Middle East Technical University, Ankara, Turkey, Phone: +90-312-210-2464, Fax: +90-312-210-5401, E-mail: [gmurat@metu.edu.tr](mailto:gmurat@metu.edu.tr)

### Research Highlights

- Higher asphalt content increases fatigue life of asphalt concrete
- Limestone improves thermal fatigue performance as compared to basalt aggregate
- Gradation and binder modification show no influence on thermal fatigue performance
- Constant amplitude strain loading facilitates study of thermal fatigue phenomenon

### Abstract

Thermal fatigue leads to serious degradations of structural performance and service quality of roadways. Thermal fatigue cracks occur in moderate climates, and are the result of generated cyclic thermal strains/stresses within the restrained pavement layers. In this study, an experimental setup is developed to measure the thermal fatigue resistance of asphalt concrete specimens under constant strain amplitude loading. To simulate thermal fatigue behavior of asphalt concrete, uniaxial loading is mechanically applied to achieve constant amplitude sinusoidal strains at a frequency of 0.01Hz. The results of statistical analyses indicate the asphalt content, aggregate source and asphalt binder type have the strongest effect on the thermal fatigue resistance of asphalt concrete.

Keywords: thermal fatigue resistance; asphalt concrete; thermal expansion coefficient; strain loading.

## 1. Introduction

Thermal cracking can cause considerable deteriorations in the structural and functional performance of asphalt concrete pavements. Thermal stress developed in asphalt concrete is attributed to the volume change characteristics of the mixture, which is defined by its thermal contraction/expansion behavior [1]. Temperature differentials produce thermal stresses because of the restraint due to friction between asphalt concrete layer and its underlying layer [2]. Thermal stresses are generated and eventually cause top-to-bottom cracking in the surface course. The cracks in the surface course, if not rehabilitated, can lead to severe structural problems and loss of service quality of roadways. Because of their significant impact on pavement performance, thermally induced cracks have drawn the attention of many pavement engineers in the last decades. Thermal cracking manifests itself in two ways: thermal fatigue cracking and low temperature cracking [3]. The former is the result of cyclic thermal changes within the pavement and the latter can result from a single drop in air temperature, which is low enough to generate thermal stresses that exceed the tensile strength of asphalt concrete. In either case, the thermal coefficient of asphalt concrete can be used for estimating the total volume change of the surface course under temperature differentials and hence generated thermal stresses.

Thermal fatigue cracking of asphalt concrete has been under observation since mid-seventies [4]. The main reason for development of sever transverse cracks in west Texas was attributed to thermal fatigue cracking [4]. To observe the factors affecting this phenomenon, it is possible to apply thermal cycles on asphalt concrete specimens in the laboratory. However, due to the low

thermal conductivity of asphalt, this process will take a long testing time and high experimental costs [5]. Another way of considering thermal fatigue in pavement design is to use numerical models for estimating the time series of temperature and computing the thermally induced strains [6]. It is also believed that the thermal fatigue cracking in asphalt concrete is dominated by high cyclic strain/stress levels induced in the flexible pavements rather than merely being controlled by the frequency of thermal cycles [7]. Thermal fatigue occurs in the flexible pavements under very low loading frequencies; nonetheless, it is possible to mechanically simulate this phenomenon in the laboratory at relatively higher frequencies [8]. It is worth noting that the simulated thermal frequencies in the laboratory are still much smaller than the frequencies (10-50 Hz) related to the load-associated fatigue [9], [10]. As a result, only a few studies concerning the thermal fatigue were conducted in the laboratory through simulated mechanical application of thermal cycles at fairly low frequency levels; these studies were performed at constant strain modes and temperatures by using either two-point [8] or four-point bending beam fatigue tests [11]. In the field, however, the thermal fatigue damages the asphalt concrete course in an expansion-contraction manner along the center line of the pavement [7]; to the best of our knowledge, this type of distress has not ever been simulated in the laboratory through the application of uniaxial cyclic loads. Since it is believed that the thermal fatigue occurs in the temperature range of  $-7^{\circ}\text{C}$  to  $21^{\circ}\text{C}$  [4], the constant temperature at which this type of distress is simulated should be within the mentioned range. It should be kept in mind that selection of a constant temperature close to the lower limit will result in a brittle fatigue behavior and selecting a temperature close to the upper limit causes the fatigue behavior to be dominated by relaxation [12].

It is known that aggregate type together with different gradations, asphalt type, asphalt content and modification affect fatigue life [13] thermal cracking resistance of asphalt concrete [14]. In terms of aggregate gradation, it is believed that gap-graded aggregates outperform the dense graded ones in the context of thermal fatigue performance [11]. In addition, if the degree of interlock in aggregate structure increases, it can improve the thermal strength of asphalt concrete [15]. As for the asphalt type, higher penetration grades result in sustaining more number of cycles before failure [16]. Binders with lower stiffness cause the asphalt concrete to better resist against thermal cracking [17]. If the asphalt content increases in the asphalt mixture, its resistance against thermal fatigue cracking improves proportionately [8]. In terms of modification, it is believed that if modifiers are added to binder they can increase the thermal fatigue life of asphalt concrete [11]. The wax crystallization in the bitumen microstructure was also found to be important to develop thermal fatigue in the binder domain of asphalt concrete [11].

In this study, in addition to testing the beam specimens consisting of different mixture variables, a thermal stress restrained specimen test (TSRST) setup was revised to determine the thermal fatigue resistance of asphalt concrete specimens through the application of uniaxial loads at a constant temperature. Then, three response variables were defined to characterize the thermal fatigue resistance of each specimen. Finally, statistical analyses were conducted to determine the significant mixture design parameters for the thermal fatigue resistance of test specimens. We hope that the results of this study will help mitigate the thermal fatigue cracking in flexible pavements; first by identifying the best mix design variables used in this study, and then by providing a new rubric for mechanical simulation of thermal fatigue cracking in the laboratory.

## 2. Materials and methods

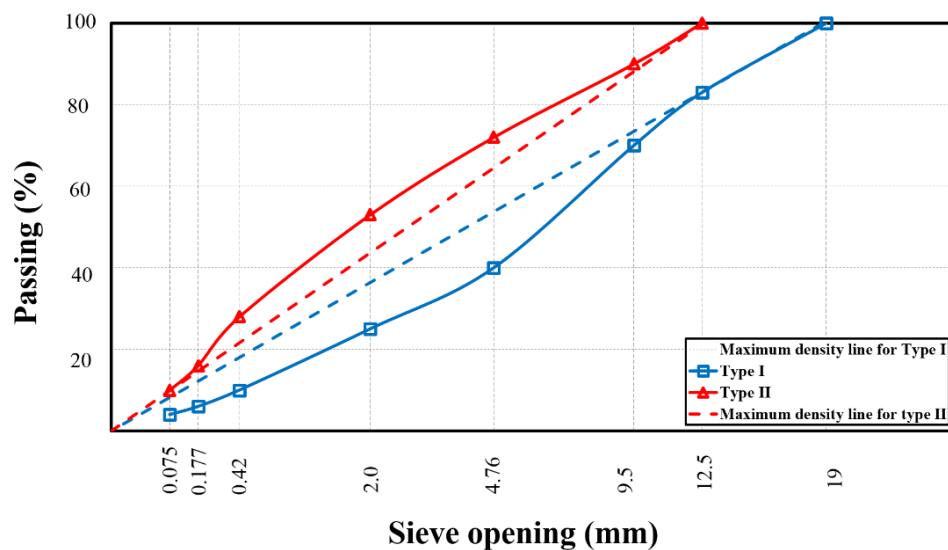
This research highlights the influence of different mixture components on the thermal fatigue behavior of asphalt concrete. The mixture design variables used in this study consisted of two types of aggregate with two gradations; two types of asphalt grade (Table 1 and Fig. 1); and three asphalt contents: optimum and the optimum  $\pm 0.5\%$ . Some of the binders used were modified with SBS and the rest were left as virgin.

**Table 1**  
Properties of aggregate and asphalt binder.

Aggregate	Specific gravity	Absorption (%)	LA abrasion (%)
Limestone	2.75	1.45	28
Basalt	2.93	1.00	15

PG grade	Penetration value (0.1mm)	Specific gravity (g/cm <sup>3</sup> )	Penetration grade
PG64-22	54	1.025	50/70
PG58-22	73	1.034	70/100



**Fig. 1.** Aggregate gradations.

After preparation of the test mixtures, they were age-hardened for three hours in the oven for the sake of achieving short term aging; then, they were compacted using a French (LCPC) slab compactor. After the compaction process, prismatic beam specimens with dimensions of  $50 \times 65 \times 250$  mm were cut out of the slabs using a diamond saw. After the cutting process, a portion of the specimens were used in a different testing program investigating the thermal fracture behavior of asphalt concrete. The remaining specimens were, however, maintained in the laboratory at ambient temperature for 5 years to be tested for the thermal fatigue resistance. This long period let the specimens be naturally age-hardened rather than under accelerated oven aging. Previous studies indicate that the thermal fatigue cracking of asphalt concrete is not a viable mode of distress unless it is age-hardened [5]. After the long-term aging process, the specimens were glued at both ends to steel platens using a high strength epoxy, and then installed into the TSRST device for the measurement of their thermal properties, i.e., thermal coefficient and subsequently thermal fatigue resistance.

In this study, along with preparation of the test specimens, the most frequent daily temperature range during the last 13 years was determined for the city of Ankara, and a TSRST machine was calibrated to measure thermal coefficient, and thermal fatigue resistance of each beam specimen. The thermal coefficients were measured to calculate the amplitude of cyclic thermal strains; such way of calculating the cyclic strains – for each specimen based on its own thermal volumetric contraction - was one of the novelties of this study. These strains were mechanically applied to each specimen for the purpose of evaluating its thermal fatigue performance at the selected frequency and the test temperature. Mechanical simulation of cyclic thermal stresses at the laboratory environment was another novelty of this research. The TSRST machine (Fig. 2) was fabricated from a steel frame and for ensuring insulation against heat loss,

its internal walls were lined with a foam material of 6 cm thickness. The load cell was also insulated with the same foam material of at least 20 cm thickness from the cooling section of the chamber. A computer and a data acquisition system were connected to the TSRST machine in order to control the tests and record the data during the experiments. To control and record the surface temperature, 4 resistance temperature detectors (RTD) were attached on each surface of the beam specimens. A probe RTD was also fixed inside a dummy specimen for measuring the core temperature during the tests.

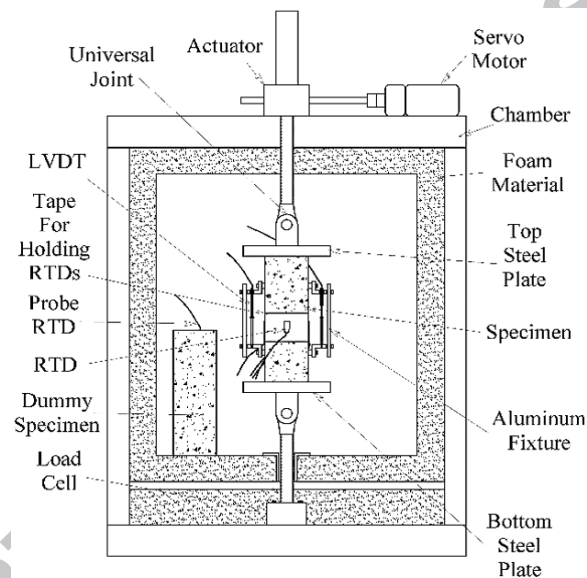


**Fig. 2.** The schematic of the TSRST machine used for measuring the thermal coefficients and thermal fatigue performance of asphalt concrete specimens.

### 2.1. Selection of the temperature range to calculate strain amplitudes

Because of daily cyclic temperature changes, flexible pavements like the other types undergo thermal fatigue cracking during their service lives. For simulating this type of distress, it was necessary to find a temperature range at which this type of distress could be evaluated in the laboratory. As a result, for investigating the effect of thermal fatigue in flexible pavements, the weather data - recorded during past 13 years - for the city of Ankara were obtained from the

Weather Bureau of Turkey. The data were then analyzed to find the frequency of temperature differentials only between  $-7^{\circ}\text{C}$  and  $+21^{\circ}\text{C}$ , a temperature range at which thermal fatigue may occur [4]. For the thermal fatigue tests, the temperature differential ( $\Delta T = 10^{\circ}\text{C}$ ) with the highest frequency was selected to compute the strain amplitudes (Fig. 3). The frequency of temperature ranges more than  $10^{\circ}\text{C}$  is also significant; however, because of the long test durations needed in thermal fatigue tests, only a single temperature differential had to be considered in the experiments.

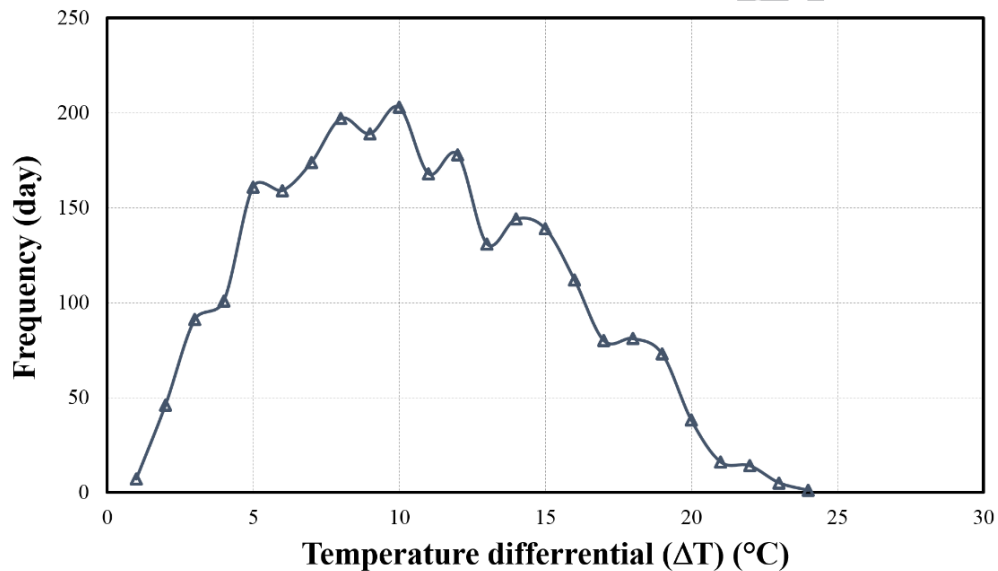


**Fig. 3.** Weather data analyzed for the city of Ankara to identify the most frequent daily temperature cycle.

## 2.2. Measurement of thermal coefficients of test specimens

To measure the thermal coefficients, the beam specimens stuck between the steel platens were mounted in the TSRST machine and were conditioned at  $15^{\circ}\text{C}$  for three hours to achieve thermal equilibrium [18]. After the preconditioning period, the environment temperature was dropped at the rate of  $10^{\circ}\text{C}/\text{h}$  starting from  $15^{\circ}\text{C}$  and ending at  $-25^{\circ}\text{C}$ . The selected temperature reduction rate was slow enough to ensure uniform temperature changes within the specimens [19]. During

the tests, the axial deformation and the measured temperatures from each RTD were logged in every 30 seconds.

To determine the thermal fatigue resistance of the specimens under constant amplitude sinusoidal loading, at first the thermal coefficient of each specimen had to be measured, so that the strain amplitudes could be calculated for a temperature differential of 10°C, as described in the above section. To achieve this, the strain and the temperature data were fitted to a five-parameter model (Eq. (1)) using the least square method [20]–[22].

$$\varepsilon_l = \frac{\Delta_l}{l_0} = C + \alpha_g(T - T_g) + R(\alpha_l - \alpha_g) \ln \left[ \exp \left( \frac{T - T_g}{R} \right) \right] \quad (1)$$

where:  $\varepsilon_l$  = linear strain at temperature  $T$ ;  $C$  = intercept constant of the model;  $T_g$  = glass transition temperature;  $R$  = constant defining the curvature;  $\alpha_l$  = thermal expansion coefficient for  $T > T_g$ ; and  $\alpha_g$  = thermal expansion coefficient for  $T < T_g$ .

During the thermal coefficient measurements, it had to be kept in mind that the thermal behavior of asphalt mixture can transform from rubbery into glassy state, as characterized by the existence of a glass transition temperature [23]. For example, in Fig. 4, there is a slight curvature at -12°C indicating the existence of a glass transition point in the applied temperature range. In this case, thermal coefficient must be calculated above and below the glass transition temperature, as indicated by the  $\alpha_g$  and  $\alpha_l$  in Eq. (1), respectively. Because of the selected temperature range (10°C), and the test temperature (5°C) in the thermal fatigue testing, Eq. (1) was used to calculate only the thermal coefficients falling above the glass transition temperature.

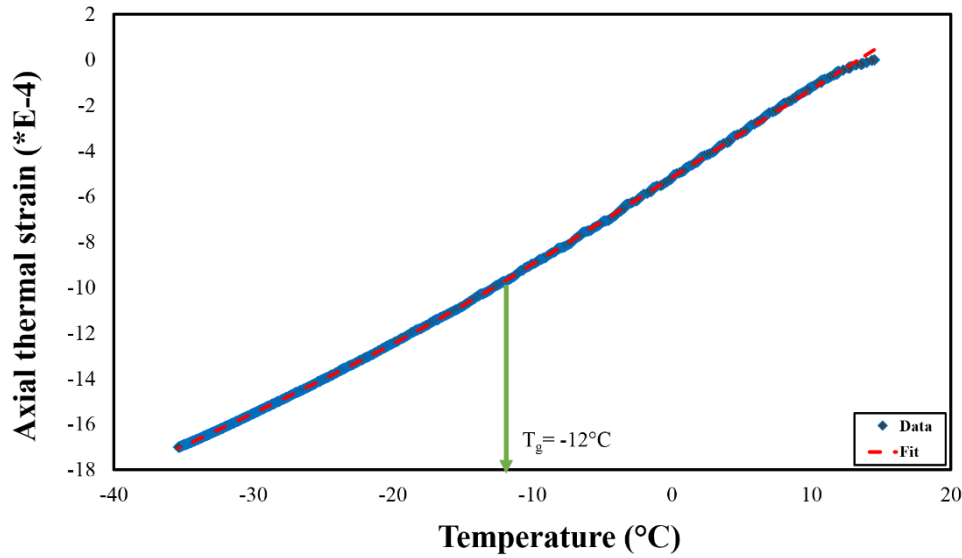


**Fig. 4.** The data recorded for one of the specimens during the measurement of thermal coefficients.

After measuring the thermal coefficients, thermal strains were calculated using Eq. (2). Table 2 lists the calculated maximum thermal strains that had to be applied on beam specimens during cyclic loading test.

$$\varepsilon = \alpha_{\text{asphalt}} \Delta T \quad (2)$$

where:  $\varepsilon$  = thermal strain at the selected temperature range;  $\alpha$  = thermal coefficient of contraction for beam specimens; and  $\Delta T$  = temperature differential, for which the strain magnitudes are calculated.

Based on the calculated strains from Eq. (2), the maximum and minimum strain levels defining the strain amplitude were chosen. In this study, it was assumed that the minimum strain level is zero implying a complete strain reversal, only at the initial cycle, for each load application. The maximum strain levels, however, were obtained with the aid of Eq. (2), for the selected temperature differential of 10° C. Fig. 5 shows the applied sinusoidal (0.01Hz) strain waveform as defined by the max. strain  $\varepsilon_{\text{max}}$ , min. strain  $\varepsilon_{\text{min}}$ , and the loading frequency  $f$ .

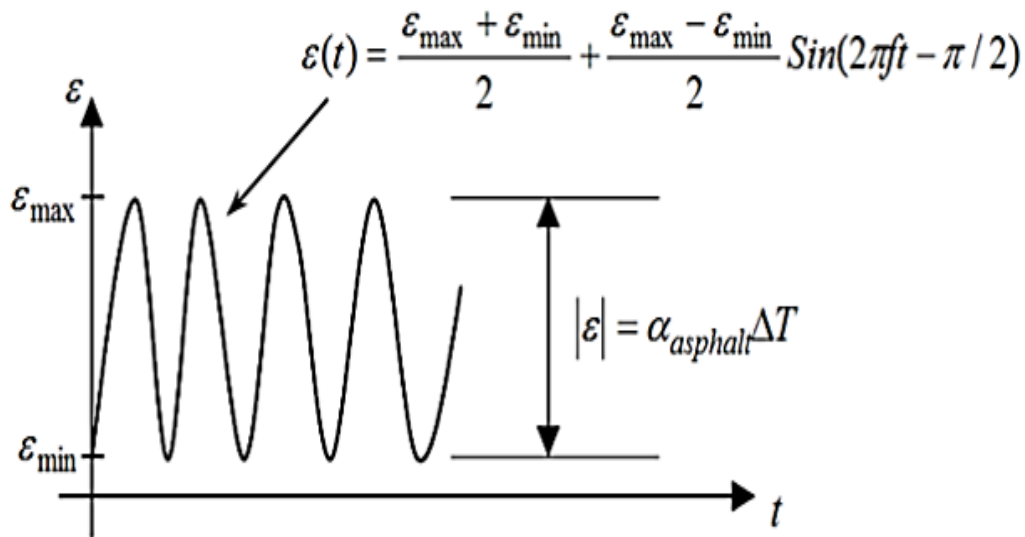


Fig. 5. Waveform for the constant amplitude sinusoidal strain loading.

It is worth noting that simulating thermal fatigue in asphalt concrete by applying uniaxial cyclic loads at the low loading frequency of 0.01Hz was one of the greatest novelties of this study.

**Table 2**

Measured thermal strains.

Specimen code	Thermal strain ( $\mu\text{m/m}$ )	Specimen code	Thermal strain ( $\mu\text{m/m}$ )
LF54ZO	333	LF73ZO-	407
LF54ZO	298	BF54ZO+	361
LF54ZO+	379	BF54ZO+	385
LF54ZO+	380	BC73ZO-	386
LC54SO-	347	BC73ZO-	384
LC54SO-	337	BC73ZO-	387
LF54SO+	374	BF73ZO+	388
LF54SO+	377	BF73ZO+	384
LF54SO+	367	BF73ZO-	305
LF73ZO	355	BF73ZO-	355
LF73ZO	382	BF73ZO-	376
LF73ZO	364	BC73SO+	444
LF73ZO-	385	BC73SO+	422

Note: B = basalt and L = limestone; C = coarse gradation and F = fine gradation; 54 = asphalt penetration value of 54(0.1mm) and 73 = asphalt penetration value of 73(0.1mm); S = asphalt modified with SBS and Z = no asphalt modification used; and O = optimum asphalt content, O- = asphalt content 0.5% less than the optimum and O+ = asphalt content 0.5% more than the optimum.

After completion of thermal fatigue tests, stiffness reduction path for each specimen was calculated by dividing peak-to-peak stress (Fig. 6a) by peak-to-peak strain (Fig. 6b) to achieve the continuous monitoring of stiffness values [24] as a function of loading cycles. In this phase, a separate algorithm was developed in the Matlab<sup>®</sup> environment to detect the correct peak to peak stress/strain of each loading cycle (see the red circles in Fig. 6). Note that Fig. 6a and Fig. 6b only present a portion of data used for calculating the stiffness, otherwise the peaks and cyclic patterns could not be detectable, if all the gathered data, for the complete duration of the test, were presented in the graph.

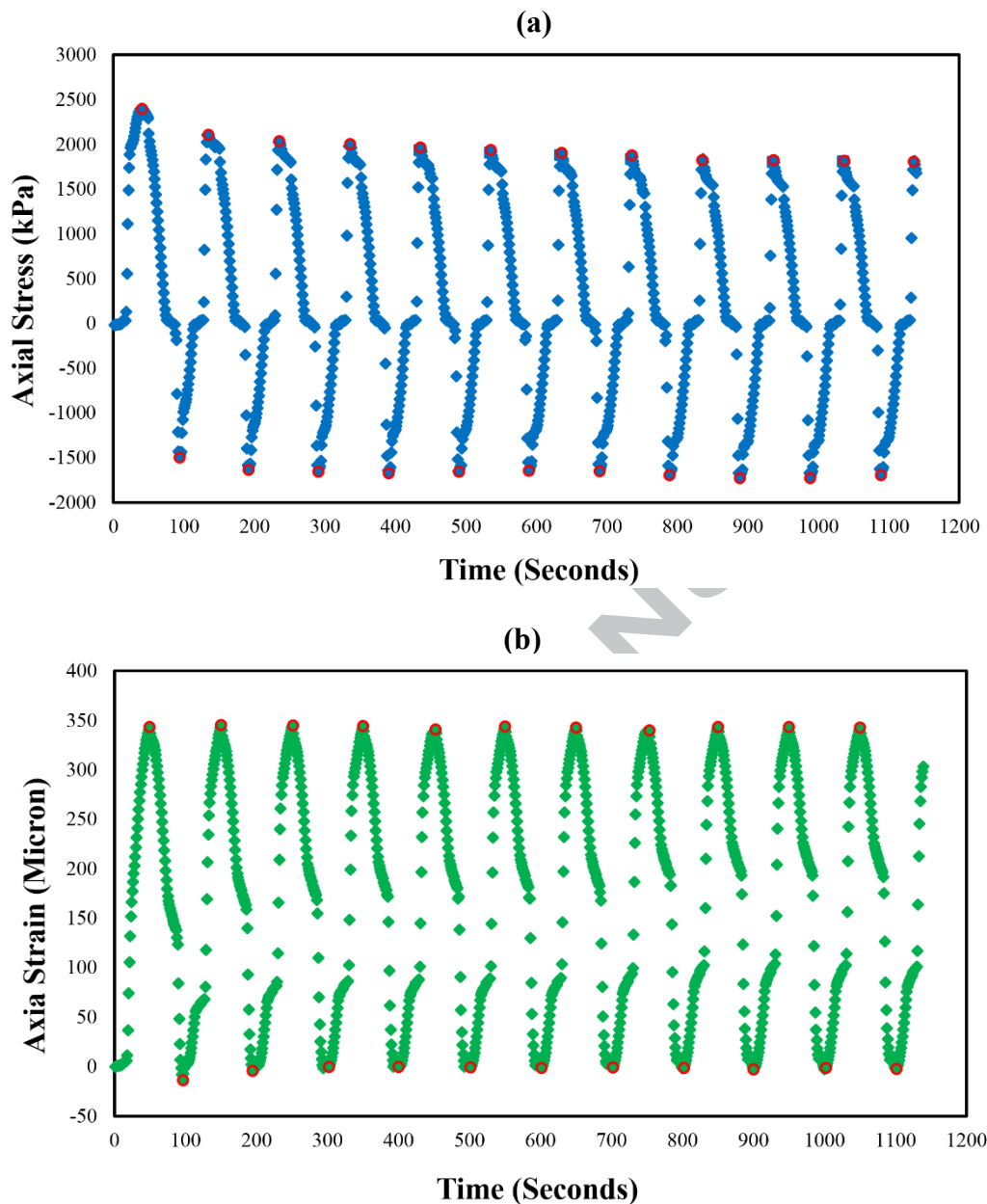


**Fig. 6.** Sample data gathered during the first 1200 seconds (i.e., 12 cycles) for calculating stiffness: (a) peak-to-peak stress data, and (b) peak-to-peak strain data.

After calculating and finding the stiffness paths, thermal fatigue resistance of each specimen was evaluated which was based on three selected response parameters: (a) 35% reduction in stiffness, (b) 50% reduction in stiffness and (c) stiffness reduction rate [8].

### 3. Data analysis

#### 3.1. Number of load cycles to achieve 35% reduction in stiffness

In conventional load-associated fatigue tests, with a frequency range applied between 10-50 Hz, the criteria for ending the tests is either 50% reduction in stiffness or when the specimen breaks [25]. However, in this study, due to the low frequency loads applied, it may not be feasible to carry on the tests until a 50% reduction in stiffness is achieved. As a result, the tests were continued until 72 hours for any specimen that did not break or fail due to approaching to 50% of its initial stiffness. Within this 72-hour time window, most of the specimens generally approached to stiffness reductions in the range of 35-50%. In the testing program, all of the test specimens could reach to 35 % reduction in the stiffness, and hence the number of load cycles at 35% stiffness levels was selected as one of the response parameters in the statistical analyses. Fig. 7 presents the stiffness reduction paths for three different specimens. As it can be seen in the figure, the paths – not being S-shaped – represent the existence of uniform strain fields within the prismatic beam specimens [16].

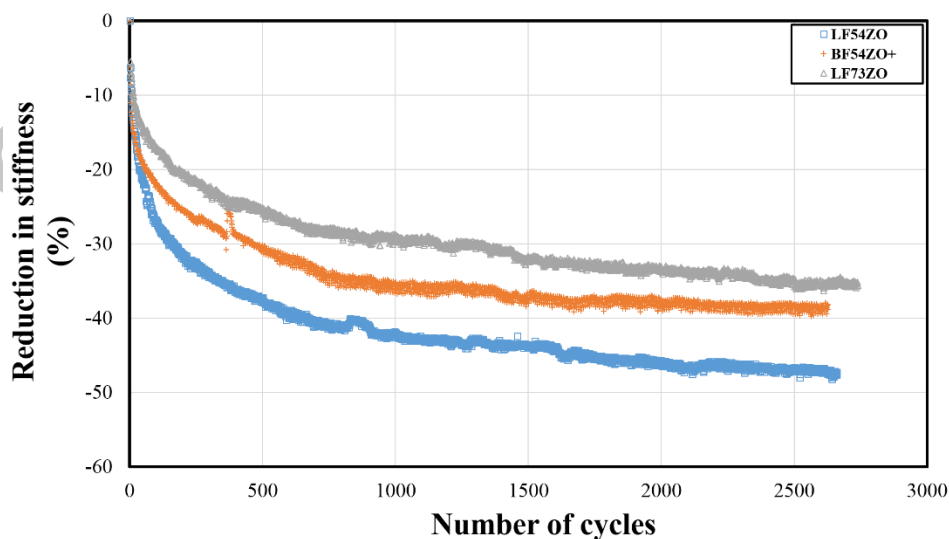


Fig. 7. Stiffness reduction paths calculated for three different specimens.

### 3.2. Estimating number of cycles to 50% reduction in stiffness using a power model

Along with evaluating the fatigue life at 35% reduction in stiffness, it was decided to extrapolate the number of cycles to 50% reduction in stiffness using a power model conventionally used for modelling the traffic load-associated fatigue:

$$S = aN^b \quad (3)$$

where:  $S$  = stiffness at  $N^{\text{th}}$  cycle; and  $a$ ,  $b$  = fatigue constants.

For fitting the power model to the data, the stiffness reduction and the number of cycles were plotted in a log-log scale for each specimen (Fig. 8), so that a portion representing the real fatigue behavior, under big constant amplitude cyclic strains, could be identified [8].

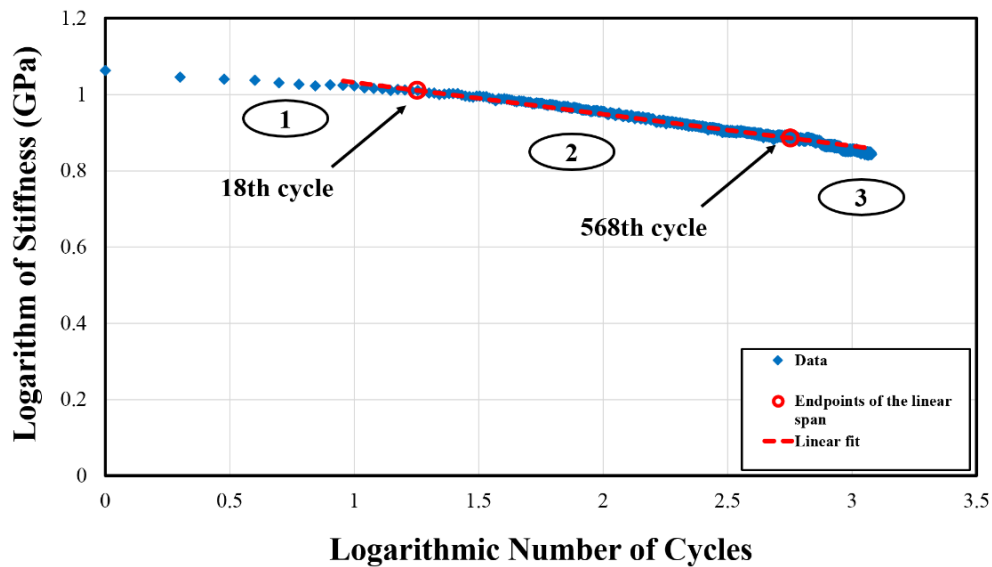


**Fig.8.** The data of stiffness versus number of cycles in a log-log scale.

In Fig. 8, the first portion is representative of an accelerating rate of reduction in stiffness which is due to the drastic changes in aggregate skeleton in the first few cycles [8]; these changes are because of the big amplitude of the constant cyclic strains that were applied on the

test specimens. The third part of the graph (i.e., region 3), in which the rate of stiffness reduction accelerates after a steady stage, is attributed to the rapid crack growth within the specimen [26].

The data plots in the log-log scale were observed visually to find a span representing the selected number of cycles belonging to the linear region. However, to exactly detect the location of the linear span, a code was written in the Matlab® environment to facilitate the fitting process. As it can be seen in Fig. 8, the red line which is fitted to the data between the two circles represents the best linear fit for the selected fatigue data.

After finding the best linear region (i.e., the region representing the real fatigue behavior [8] with a moderate rate of loss in stiffness [26]), a power model (Eq. 3) was fit to the aforementioned region - between the selected points (Fig. 9) -, so that the number of cycles to reach 50% reduction in stiffness could be extrapolated for each specimen type.

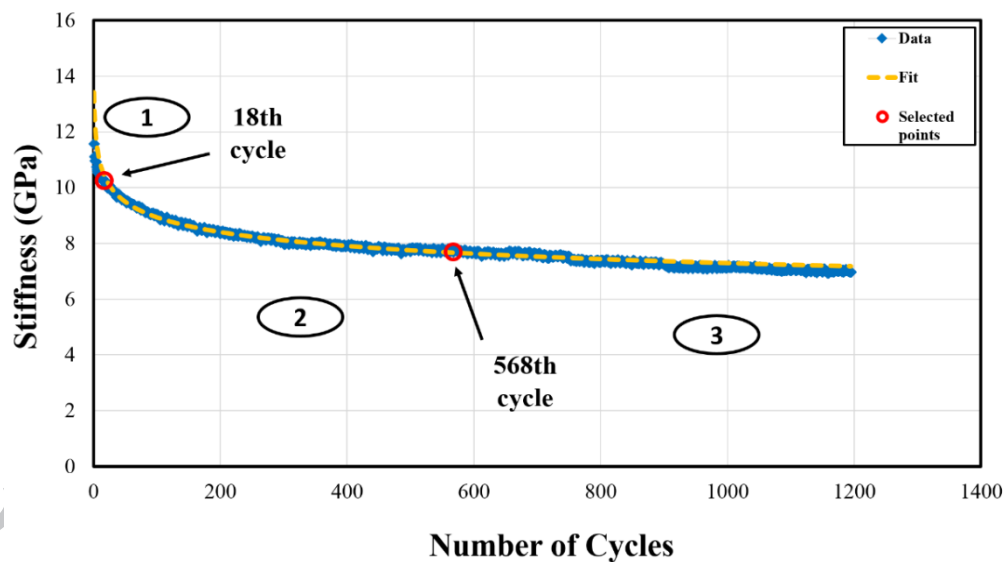


**Fig.9.** Power model fitted to the portion of data representing the fatigue behavior, i.e., the region between the selected points.

### 3.3 Stiffness reduction rate

An alternative approach for estimating the thermal fatigue life of asphalt concrete is finding the slope, i.e., the stiffness reduction rate, of the linear line fitted to the log-log scale data (see Fig. 8). The slope of fitted linear line is representative of micro-crack growth development rate, or in other words the thermal fatigue life of asphalt concrete [8]. As a result, the stiffness reduction rate was also calculated for all the specimens to give an estimate of thermal fatigue life of the asphalt concrete specimens studied in this research.

## 4. Results and discussion

Statistical analysis of variance test (ANOVA) was conducted on the selected response parameters characterizing the thermal fatigue performance of asphalt concrete specimens. ANOVA was performed for each parameter at 95% confidence level, and the results are presented in Table 3.

**Table 3**

Results of ANOVA analyses for the selected response parameters.

Mixture design variable	35% reduction in stiffness	50% reduction in stiffness	Rate of stiffness reduction ( $\alpha$ )
Aggregate type	0.069	0.053	0.002
Gradation	0.618	0.528	0.333
Asphalt type	0.062	0.584	0.084
Modification	0.321	0.105	0.641
Asphalt content	0.005	0.023	0.061

Significant mixture design variables influencing the thermal fatigue performance of asphalt concrete specimens can be identified by observing the probability ( $p$ ) values for the selected confidence interval of  $(1-\alpha) = 0.95$ . Table 3 presents the mixture design variables, P-values and selected response parameters. The first response parameter used was the number of load

applications producing 35% reduction in stiffness. Note that the significant mixture design variable for this response parameter is the asphalt content with a probability level of 0.005. However, the aggregate type and asphalt binder may contribute to the stiffness reduction at the selected stiffness reduction level. The graphical analysis for asphalt content (Fig. 10) shows optimum minus 0.5% by O- through optimum plus 0.5% by O+. Increasing the binder content increases the fatigue life of asphalt concrete. It is believed that the amount of air voids in the mixture affects the age hardening of the asphalt. If the asphalt content is increased, the binder will become less prone to age hardening and hence the asphalt concrete sustains more thermal cycle before failure [6]. The other reason for this behavior could be attributed to the increased bonding between the aggregates when higher asphalt contents are used in the mixtures.

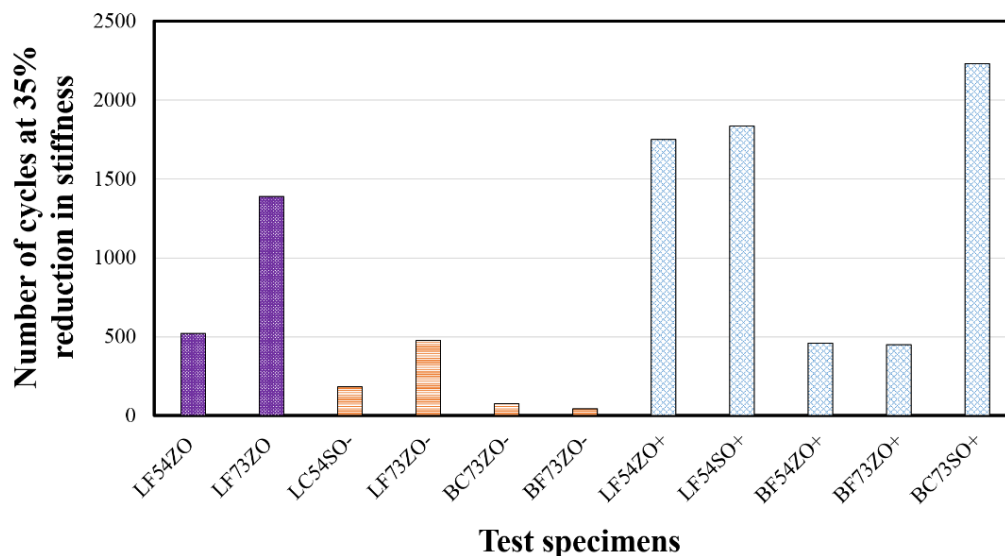


**Fig. 10.** Average number of cycles to 35% reduction in stiffness calculated for asphalt content.

The effect of mixture design variables on the thermal fatigue resistance for 50% reduction in stiffness can also be observed from second column of Table 3. As for the first response parameter, asphalt content again is the most significant parameter affecting the fatigue resistance of the specimens with a probability level of 0.023. This obtained P-value is slightly lower than

for the first response parameter; however, the impact of asphalt content in fatigue performance again remains for the test specimens. The graphical analysis of this response parameter in Fig. 11 also shows a similar trend, as in Fig. 10, except for one of the specimens (BF54ZO+).

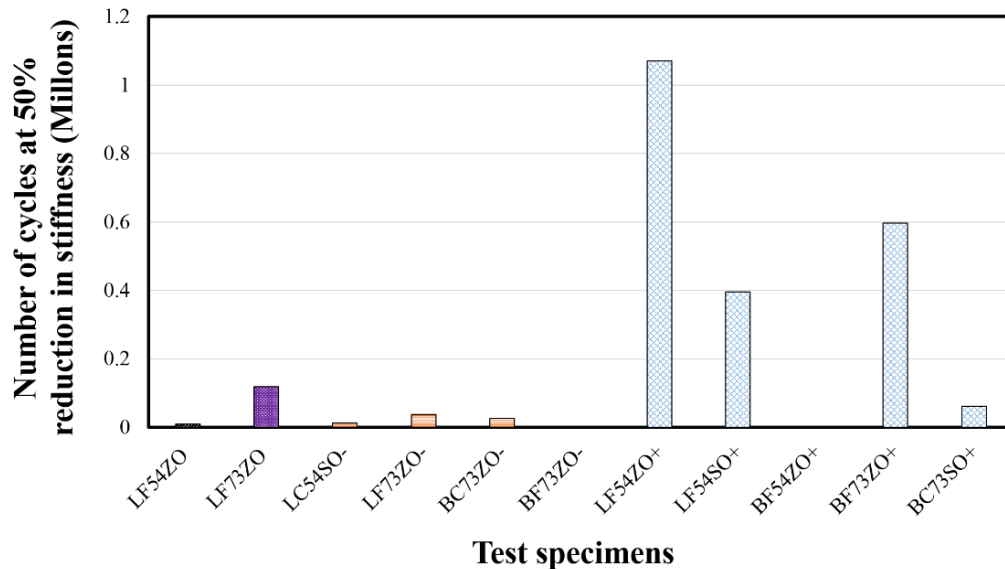


**Fig. 11.** Average number of cycles to 50% reduction in stiffness calculated for asphalt content.

The third response parameter (a) was the slope of the stiffness-number of load cycles relationship in the log-log scale, and indicates the rate of reduction in the stiffness of the specimens. The results of ANOVA for this parameter can be observed in Table 3. Note that the aggregate type is the most significant factor for the fatigue resistance of the test specimens with a probability level of 0.002. The aggregates used in the testing program included limestone and basalt, which normally display significant mixture performance under conventional load-associated fatigue tests performed under high frequencies. However, it appears that aggregate type became a dominating mixture factor for the loading conditions under very low loading frequencies as applied in this testing program. The rate of reduction in stiffness was higher for basalt aggregate than for limestone (Fig. 12). This was expected because limestone bonds better with binder than does basalt, and therefore leads to a higher tensile strength of the mixture.

Similar findings were also found in previous studies when the two aggregates were evaluated under low temperature cracking [14].

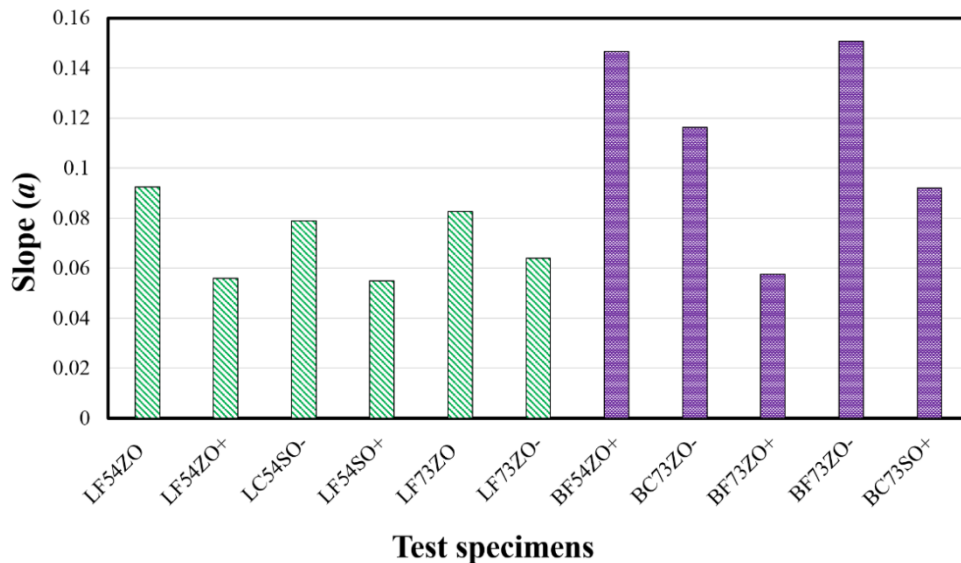


**Fig. 12.** Average rate of reduction in stiffness calculated for aggregate type.

## 5. Conclusions

In this study, in order to measure the thermal fatigue resistance of asphalt concrete specimens, a TSRST machine was revised to measure thermal fatigue performance of specimens under constant amplitude sinusoidal loading. The maximum strain levels used for performing tests on specimens were determined by the measured thermal coefficients obtained for each specimen based on a constant temperature differential of 10 °C. The data obtained from the thermal fatigue tests were statistically analyzed for the selected response parameters to identify the effect of mixture design variables on the thermal fatigue performance of the test mixtures. The results of analyses led to the following outcomes:

- Increasing asphalt content resulted in improved thermal fatigue resistance as indicated by the increased load cycles to both 35% and 50% reduction in the stiffness of the specimens.  
Asphalt content is a significant mixture design factor for the thermal fatigue performance of the mixtures. Increasing the asphalt content increases the thermal fatigue life of flexible pavements as the way it increases the traffic load-associated fatigue life.
- Limestone resulted in sustaining higher number of load cycles than for basalt for the same reduction level in mixture's stiffness. Therefore, aggregate type is a significant factor affecting the thermal fatigue resistance.
- Although the statistical analyses did not indicate aggregate type as a significant factor for 35% and 50% stiffness reduction levels, it seems that the next important mixture design variable for thermal fatigue performance will be aggregate type given the probability levels calculated for this factor. Hence, further research is needed to investigate the effect of aggregate type on thermal fatigue performance of asphalt concrete.
- Uniaxial application of cyclic loads seems to be a trustable method for measuring the thermal fatigue resistance of asphalt concrete beam specimens, since the stiffness reduction path obtained were normal. Moreover, the thermally induced contraction and expansion in the field occurs along the centerline of the pavement.
- Using a close-to-reality simulation for investigating the effect of mixture design variables affecting the thermal fatigue performance of asphalt concrete, can help make long-lasting flexible pavements that are resistant to thermal changes in the field.

## Acknowledgments

This study was conducted at Middle East Technical University (METU), and all the tests were performed at Transportation Laboratory (TL) of METU. The authors would like to express their sincere gratitude to METU for providing the laboratory, equipment and all the means for accomplishing this study. The authors would also like to thank Mr. Ahmet Sağlam, METU TL technician, for his assistance with the lab investigations. This research did not receive any specific grant from funding agencies in the public, commercial, or not-for-profit sectors.

## References

- [1] R. L. Lytton, J. Uzan, E. G. Fernando, R. Roque, D. Hiltunen, and S. M. Stoffels, "Development and validation of performance prediction models and specifications for asphalt binders and paving mixes. SHRP-A-357," p. 552, 1993.
- [2] A. Arabzadeh, "The influence of different mixture design variables on thermal fatigue cracking of asphalt concrete pavements," Middle East Technical University, 2015.
- [3] Y. Zhu, E. V. Dave, R. Rahbar-Rastegar, J. S. Daniel, and A. Zofka, "Comprehensive evaluation of low-temperature fracture indices for asphalt mixtures," *Road Mater. Pavement Des.*, vol. 18, no. 4, pp. 467–490, 2017.
- [4] S. H. "Carpenter, "Thermal cracking in asphalt pavements: an examination of models and input parameters," *United States Army Corps of Engineers Cold Regions Research and Engineering Laboratory*. Hanover, NH, 1983.
- [5] N. Jackson and T. Vinson, "Analysis of thermal fatigue distress of asphalt concrete pavements," *Transp. Res. Rec. J. Transp. Res. Board*, vol. 1545, pp. 43–49, 1996.
- [6] A. Walther and M. Wistuba, "Mechanistic pavement design considering bottom-up and top-down-cracking," in *7th RILEM International Conference on Cracking in Pavements*,

- 2012, pp. 963–973.
- [7] I. Al-Qadi, M. Hassan, and M. Elseifi, “Field and theoretical evaluation of thermal fatigue cracking in flexible pavements,” *Transp. Res. Rec. J. Transp. Res. Board*, 1919(1), pp. 87–95, 2005.
- [8] A. . Gerritsen and D. J. Jongeneel, “Fatigue properties of asphalt mixes under conditions of very low loading frequencies,” in *Association of Asphalt Paving Technologists Technical Sessions*, 1988.
- [9] U. A. Mannan, M. R. Islam, and R. A. Tarefder, “Effects of recycled asphalt pavements on the fatigue life of asphalt under different strain levels and loading frequencies,” *Int. J. Fatigue*, vol. 78, pp. 72–80, 2015.
- [10] J. S. Daniel, M. Corrigan, C. Jacques, R. Nemati, E. V. Dave, and A. Congalton, “Comparison of asphalt mixture specimen fabrication methods and binder tests for cracking evaluation of field mixtures,” *Road Mater. Pavement Des.*, pp. 1–17, 2018.
- [11] A. L. Epps, “An approach to examine thermal fatigue in asphalt concrete,” *J. Assoc. Asph. Paving Technol.*, vol. 68, pp. 319–348, 1999.
- [12] Mo. Bazzaz, M. K. Darabi, D. N. Little, and N. Garg, “A straightforward procedure to characterize nonlinear viscoelastic response of asphalt concrete at high temperatures,” *Transp. Res. Rec. J. Transp. Res. Board*, vol. 2710, no. 3704, pp. 1–20, 2018.
- [13] M. Sol-Sánchez, A. Fiume, F. Moreno-Navarro, and M. C. Rubio-Gámez, “Analysis of fatigue cracking of warm mix asphalt. Influence of the manufacturing technology,” *Int. J. Fatigue*, vol. 110, pp. 197–203, 2018.
- [14] A. Qadir, “Investigation of low temperature cracking in asphalt concrete pavements,” Middle East Technical University, 2010.

- [15] Y. Q. Tan, "Effect of aggregate grading on low temperature cracking resistance in asphalt mixtures base on mathematical statistics," in *6 th RILEM International Conference on Cracking in Pavements*, 2008, pp. 387–394.
- [16] R. Lundstrom, H. Di Benedetto, and U. Isacson, "Influence of asphalt mixture stiffness on fatigue failure," *J. Mater. Civ. Eng.*, vol. 16, no. 6, pp. 516–525, 2004.
- [17] E. R. Brown, P. S. Kandhal, F. L. Roberts, Y. R. Kim, D. Y. Lee, and T. W. Kennedy, *Hot Mix Asphalt Materials, Mixture Design, and Construction*. Lanham, MD: NAPA Research and Education Foundation, 2009.
- [18] A. Arabzadeh and M. Güler, "Influence of mixture design variables on thermal coefficient of asphalt concrete," in *Proceedings of Conference on Advances in Civil Engineering*, 2014, pp. 1–6.
- [19] D. Jung and T. S. Vinson, "Low temperature cracking resistance of asphalt concrete mixtures," *J. Assoc. Asph. paving Technol.*, vol. 62, pp. 54–92, 1993.
- [20] P. K. Das, D. Jelagin, B. Birgisson, and N. Kringos, "Micro-mechanical investigation of low temperature fatigue cracking behavior of bitumen," in *7th RILEM international conference on cracking in pavements*, 2012, pp. 1281–1290.
- [21] H. Tabatabaee, R. Velasquez, and H. Bahia, "Modeling thermal stress in asphalt mixtures undergoing glass transition and physical hardening," *Transp. Res. Rec. J. Transp. Res. Board*, vol. 2296, pp. 106–114, 2012.
- [22] H. Bahia, H. Tabatabaee, and R. Velasquez, "Asphalt thermal cracking analyzer (ATCA)," in *7th RILEM International Conference on Cracking in Pavements*, 2012, pp. 147–156.
- [23] H. U. Bahia and D. A. Anderson, "Glass transition and physical hardening of asphalt

- binders,” *J. Assoc. Asph. Paving Technol.*, vol. 62, pp. 93–129, 1993.
- [24] M. Arabani, S. M. Mirabdolazimi, and A. R. Sasani, “The effect of waste tire thread mesh on the dynamic behaviour of asphalt mixtures,” *Constr. Build. Mater.*, vol. 24, no. 6, pp. 1060–1068, 2010.
- [25] AASHTO, “Standard method of test for determining the fatigue life of compacted asphalt mixtures subjected to repeated flexural bending (T 321),” 2017.
- [26] F. Pérez-Jiménez, R. Botella, T. López-Montero, R. Miró, and A. H. Martínez, “Complexity of the behaviour of asphalt materials in cyclic testing,” *Int. J. Fatigue*, vol. 98, pp. 111–120, 2017.